This version is available at https://strathprints.strath.ac.uk/58597/

Micro-Indentation based study on steel sheet degradation through forming and flattening: toward a predictive model to assess cold recyclability

Javad Falsafi[*], Emrah Demirci

Wolfson School of Mechanical and Manufacturing Engineering, Loughborough University, LE11 3TU, Loughborough, UK

A B S T R A C T

Sheet metal forming has always been an important sector of the metal industry thanks to work hardening, however, a complex set of deformation entails evolution of damage in the material through the forming stages. With an outlook to cold recycling of sheet metals, this paper focuses on experimental quantification of damage and degradation in load carrying capacity due to the forming process. Assuming that cold recycling of sheet metals involves an intermediate flattening prior to the secondary forming process, the adverse effects of flattening on the material was also investigated. An industrial cold roll forming process was taken as case study. An experimental investigation using microhardness mapping on the cross-section of fold zones, in conjunction with 3D global-local FE modelling, were the basis of through-thickness damage analysis. Taking advantage of strain-hardness correlation a new method was established to extrapolate hardness for ductile damage characterization. Investigation on sensitivity of the measured microhardness to crystallographic texture and sample surface preparation backed the experimental results. The results particularly outlined the progressive decrease in load carrying capacity of material after forming and after flattening. The possibility of a secondary manufacturing process is discussed.

Keywords: Cold recycling, Microhardness mapping, Damage, Submodelling, Cold Roll Forming, FEA

1. Introduction

[*] Corresponding author:

Tel: +44 (0)141 534 5541, E-mail: falsafi.javad@gmail.com

Conventional recycling of sheet metal wastes involves melting process, however, high melting point of metals and additional processes required to get the final product, turns it into yet an energy intensive process. If these wastes can be recycled through a cold recycling/remanufacturing process, there is a potential of a high level of energy saving. Cold recycling is an emerging area mostly studied empirically (Cooper and Gutowski, 2015), in the area of sheet metals there are few studies that investigated the feasibility of cold recycling methods and processes.Takano et al. (2008) studied the possibility of cold recycling of sheet metal wastes with a focus on the deformation behaviour of flattened sheet metal waste using incremental forming to inhibit strain localization. The author showed that thickening the thinned bent corners using special incremental flattening device could restore the material to its primary forming limits.

Tekkaya et al. (2008) demonstrate remanufacturing contoured sheet metal part by applying hydro-forming. They showed that material inhomogeneity left from the primary forming process could be gotten away with, using hydroforming. They concluded that their technique is applicable for re-use of formed sheet metal parts and could potentially be used to transform car bonnets, for instance, into other useful shapes.

From mechanics of material viewpoint, sheet metal forming stages result in progressive modification of material characteristics that could lead to failure when a high level of plastic flow occurs. Evaluating the feasibility of cold recycling requires characterization of the accumulated damage and material's residual strength which has not been investigated in previous works. The present research is an effort to characterise the damage and residual strength in waste cold roll formed sheet metals. Cold Roll-Forming (CRF) is a continuous mass production forming process in which a sheet metal is gradually bent in the transverse direction into desired cross-sectional profile using series of forming rolls. This forming technology is used for wide range of applications including automobile components. However, since the sheet in bent corners undergoes large tensile and compressive deformations, it is prone to ductile damage.

In this context, to evaluate the residual load carrying capacity of formed profile, damage evolved through the thickness of bent corners was investigated. It was assumed that there would be an intermediate flattening stage before remanufacturing or secondary forming process. When subject to flattening, the material would experience further damage; therefore, the residual strength is also studied after flattening.

For this purpose amongst different techniques for damage characterization, according to in-depth comparison reported by Tasan et al. (2012) microhardness test was selected as a suitable indirect technique. In order to make a reasonable assessment, however; through thickness microhardness test on virgin material preceded the main measurements. Microhardness on virgin sheet revealed the heterogeneity

in thickness direction which should be taken into account for accurate damage characterization. Similar observation was presented in the work by Mkaddem et al. (2002).

An important part of damage characterization using hardness is to link the hardness to associated plastic strain. Extrapolation of hardness with respect to plastic strain is a common approach to linking the two as reported by Mkaddem et al. (2006) that used hardness and corresponding plastic strain taken from tensile test, and characterise damage. In the present research, for through thickness damage characterisation, where plastic strain is not measurable, this gap was bridged using finite element simulation. In a similar framework, Muller et al. (2011) demonstrated a 2D finite element analysis of V-band roll forming and used microhardness test as an experimental verification technique. They utilised an experimental graph to correlation hardness values and equivalent plastic strain distribution in cross-section.

In present research to predict the equivalent plastic strain distribution in the cross-section, FE simulation of multi stage roll forming process was carried out. With an emphasis on capturing complex cross-sectional nuances of material behaviour, a 3D global-local technique was implemented by using shell element for a global/master model, followed by submodelling of regions of interest (bent corners), using several layers of brick elements. The challenges in such modelling are partly addressed in this paper.

The main objective of this study was, investigating material residual carrying capacity after forming, and to obtain an insight to the additional degradation through flattening. Ductile damage was characterised experimentally through extensive micro-hardness tests to map out the variations in the cross section of the material in conjunction with FE simulation. These tests were preceded by through-thickness indentations on the virgin material. Further, the sensitivity of microhardness results on quality of surface finish and orientation and crystallographic texture were investigated.

This study is part of a larger framework that tends to explore the remanufacturing/cold-recycling of sheet metal products for energy saving and sustainable in manufacturing. The presented study serves as part of the picture which estimates the decrease in load bearing capacity through flattening process. To the best of authors' knowledge, the FE modelling and damage characterization technique are the novel aspects presented in this paper.

2. Finite element model

2.1. Overview

Numerical simulation of roll forming has been around for more than 3 decades now from one of the early attempts by Rebelo et al. 1992 And McClure and Li (1995), to recent works by Bidabadi et al. (2015), the prime focus of majority of these works has been identifying the links between forming process design, material behaviour and occurrence of redundant deformations.

Bui and Ponthot (2008) used an in-house code, Metafor, for 3D model with brick elements to parametrically study the influence of different forming parameters such as the forming speed, the material properties, and the friction coefficient. Zeng et al. (2009) presented process optimisation based on response surface with the spring-back angle as the objective function and maximum longitudinal strains as a constraint. Paralikas et al. (2010) optimised the inter-distance between roll stations to minimise the elastic longitudinal and shear strains as well as the strip edge wave. Wiebenga et al. (2013) presented optimisation techniques to obtain forming process station inner-distance and settings of adjustable tools stand. Joo et al. (2011) presented an effort to avoid roll forming defects and to optimise forming parameters. Safdarian and Naeini (2015), and Bidabadi et al. (2015) investigated the effects of various parameters on bowing and longitudinal strain in channel products; they investigated parameters such as bending angle increment, strip thickness, flange width of the section, web width of the section, roll stands distance, roller speed, and the friction coefficient.

Various techniques have also been reported in simulating this forming process to its complexity however two mainstream approaches can be observed in the literature. First, rotating rolls that feed the strip forward in the presence of friction as reported by Bui and Ponthot (2008), Zeng et al. (2009), Paralikas et al. 2009 and Paralikas et al. 2011. The second approach is to move the non-rotating rolls with constant speed over the material without friction. Sheu (2004) stated that the resultant motion is the same and effect of friction is insignificant, but boundary conditions are easier to specify. Bui and Ponthot (2008) in their parametric study showed that there is almost no difference between the predictions of first and second approach and friction creates mainly the forward drive Hellborg (2007) similarly concluded that friction mainly affects the predicted reaction forces in the tools in opposite direction of the travel. This technique was also reported by others such as Tehrani et al. (2006) and Guo et al. (2009).

Elements type predominantly used in the literature is shell element as reported by Park et al. (2014), Safdarian and Naeini (2015) and Bidabadi et al. (2015). Modelling of the strip using brick elements is also

4

reported in some publications including Hong et al. (2001), Bui and Ponthot (2008), Paralikas et al. 2009 and Rossi et al. (2013). Hellborg (2007) compared both element types for roll forming simulation and pointed out that, bending prediction using brick elements, require at least four elements in the thickness direction and almost four times longer CPU time compared to shell elements.

In the present paper, with the particular need for predicting through thickness plastic strain distribution, three-dimensional FE simulations of existing roll forming were carried out using MSC.Marc software package. Complete geometry of roll forming process was created (see Fig. 1). The technique adopted in this simulation was to pull the non-rotating frictionless rolls over the strip. Since the speed of CRF operations is rather moderate (i.e. 0.3 m/s in the present simulation), the kinetic energy is not significant compared to the total energy, which is mainly dominated by folding a strip. Hence, the static implicit approach was employed to simulate the CRF process in this study.

In FE simulation of sheet materials, it is common to employ shell type element to improve simulation run time. However compared to solid (brick) elements, shell elements provide limited information about through-thickness material behaviour. On the other hand, solid elements for a large simulation, with several elements through the thickness, are computationally costly. To overcome this challenge, a global-local modelling technique was implemented, in a sense that first, the master/global model was created and run using shell elements, and then in separate simulations, regions of interests were submodelled using solid elements. This approach improved the total run time by allowing running two models with faster elements or lower mesh count, instead of running one large simulation with computationally costly elements.
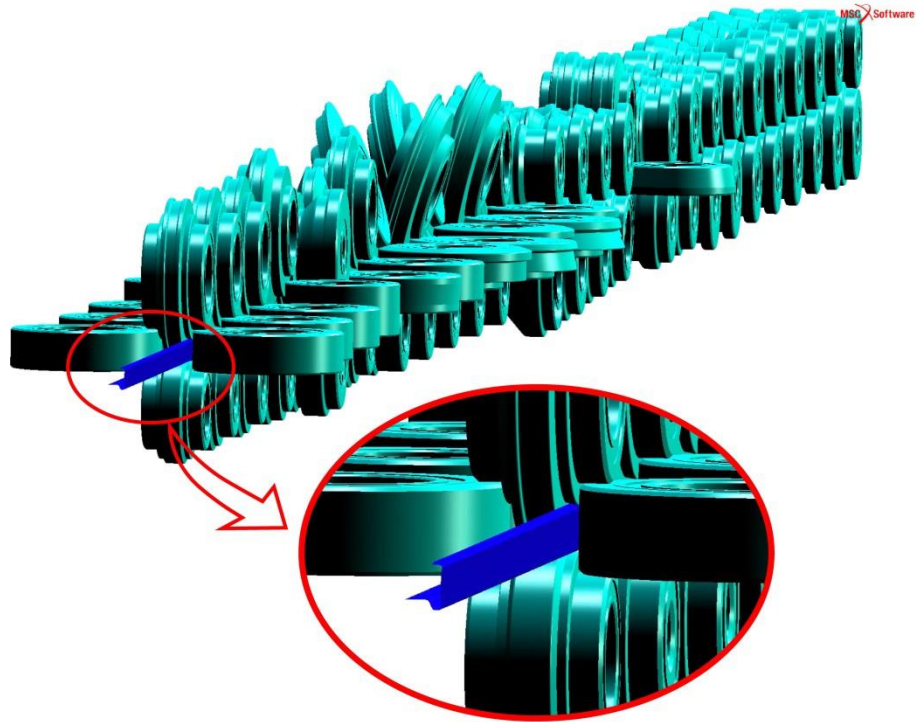
Fig. 1. 3D finite element simulation of the complete roll forming process. Half of the symmetric strip was modelled in master model.

2.2. Geometry and mesh

In master model a bilinear thick shell element 75 (MARC, 2014) was used to simulate the strip with nodes in the centre plane and 11 integration points in the thickness direction. Fig. 2 depicts the mesh in the lateral direction, was refined around fold zones, where a significant amount of plastic flow occurs. Mesh size in the longitudinal direction was quite coarse, except for a central strip with fine longitudinal mesh where the local submodels would be. The master model contains around 30000 elements.

For local submodels, the fold zones were modelled using solid elements 7 (MARC, 2014) with 10 layers of element in thickness direction. The total Number of elements in the submodels was between 2500-3500 depending on the region. Fig. 2 illustrates the half strip master model and the 4 local regions of interest. The four zones 1 to 4 were investigated experimentally as well.
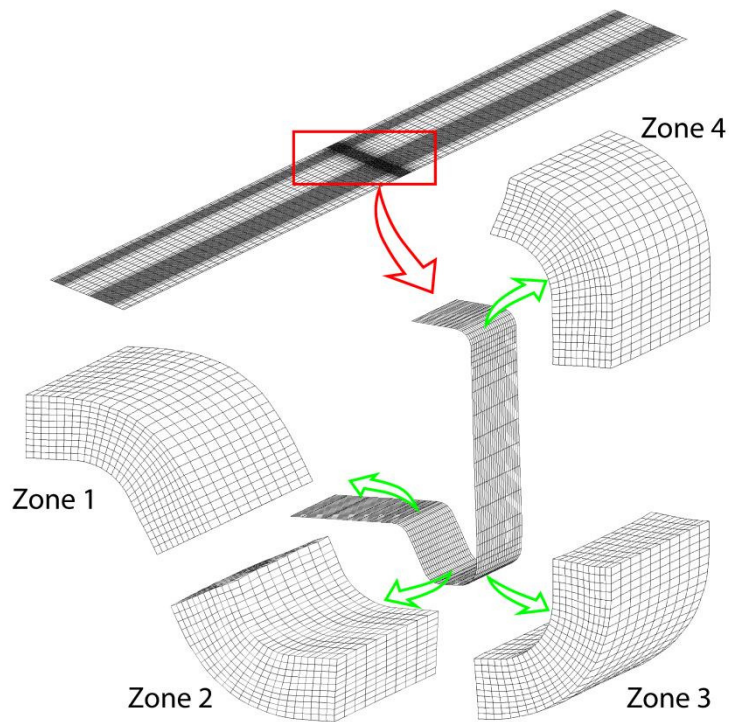
Fig. 2. Global/master model of half strip with shell element and submodels of fold zones modelled with 10 layers of solid elements.

2.3.   Contact, boundary conditions and links

To describe the contact condition and the interaction between the tools and the sheet, the analytical surface of rollers were defined as rigid bodies and a constant speed was assigned to all rollers. The material was modelled as an element-based deformable body as explained in the previous section. Friction was not considered to simplify the model as it mainly influences the reaction forces in the tools in the opposed direction of travel which is not of interest in this simulation.

In the master model, boundary conditions were applied to the front and end edge to suppress the displacement along the longitudinal direction. This was to comply with the assumption that the points on one plane with normal axis in line with the process line, remain on the same plane all through the forming process. Along the longitudinal symmetry line, the displacement perpendicular to symmetry plane was suppressed as well as rotations about the two other axes in the symmetry plane.

In the four local submodel simulation, only a GLOBAL-LOCAL type boundary condition was applied. This boundary condition establishes a link between the master model result and the local model. By defining a list of connecting nodes in local model, the kinematic boundary conditions of these nodes are automatically calculated by the software, based on the global analysis. In local models, this boundary condition was

7

applied to a line of nodes in the middle of the thickness as global model consisted of shell elements. For the mid thickness nodes to transfer this nodal data (boundary condition) to other nodes, a set of additional multi-point constraints was required, in our case RBE links. However, incorporating RBE link with mid thickness node as the reference node causes a conflict by imposing an extra constraint on top of the global-local boundary condition. The best remedy found for this conflict was to introduce one row of shell elements surrounding the brick elements. In such arrangement, the GLOBAL-LOCAL boundary condition was applied to outer edge nodes of surrounding shell elements, while the inner nodes are RBE coupled to the side nodes of the solid elements. Fig. 3 illustrates the arrangement of elements in submodels.
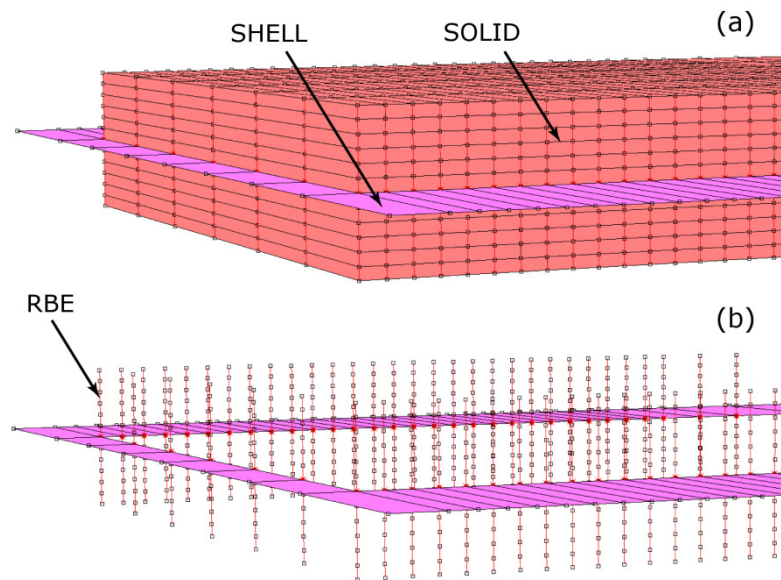

Fig. 3. Elements in submodel simulation, (b) shell elements and how their nodes are connected to those of solid elements through RBE link.

2.4. Material

The material used in the actual roll forming process was HD Galvanised structural steel S250 ZMA 275 (BS 10346:2009). Elastic-plastic model Von-Mises criteria as yield function was employed. It is recommended to use kinematic hardening for cases that material experience a reversal loading under cyclic condition, however relevant parameters for such model was not available for our material. Considering the fact that only a half cycle is involved in presented process a simplified isotropic hardening was assumed. Standard tensile test was performed to characterize material according to power law hardening formulation $\sigma = K \varepsilon^n$. The damage model introduced by Bonora (1997) was employed in the model and the associated

parameters were identified experimentally according to the method presented by Bonora et al. (2004). The summary of the material model parameters are given in Table 1.

Table 1. Summary of material model parameters in FE simulation.

HD S250 ZMA 275		
Material Model	Iso Elasto Plastic	
E	200 GPa	
υ	0.3	
σ_y	280 MPa	
K	600 MPa	
n	0.21	
Sheet thickness	1	mm

Bonora damage parameters	
ε_{th}	0.043
ε_f	0.8
D_0	0
D_{cr}	0.12
α	0.23

2.5.   Flattening

The roll forming simulation was followed by an unbending simulation, enabling us to track the variations of plastic flow in the material. This was performed in a set of separate simulations by introducing the final stage of the forming simulation of each corner as the initial condition of the corresponding flattening simulation. The initial condition takes the result file of submodelling simulation and applies the stress and strain and displacement of the material at the last time step to the flattening simulation; therefore, the material at the beginning of flattening simulation appears as bent and attributes the mechanical state of the post-forming material.

In line with the experiment, flattening was simulated by unwinding the bent material between two surfaces back to the original thickness. In practice flattening was performed by unwinding the bent corner between the two jaws of the bench vice as illustrated in Fig. 4.
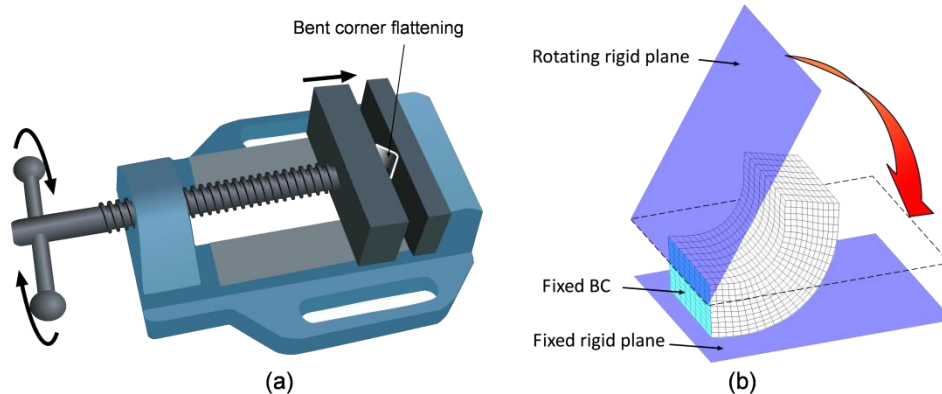
Fig. 4. Flattening process, (a) schematic of experimental flattening of bent corner using bench vice, (b) schematic of the flattening a bent corner in FEA

Example of the predicted total equivalent plastic strain after forming and flattening is shown in Fig. 5.
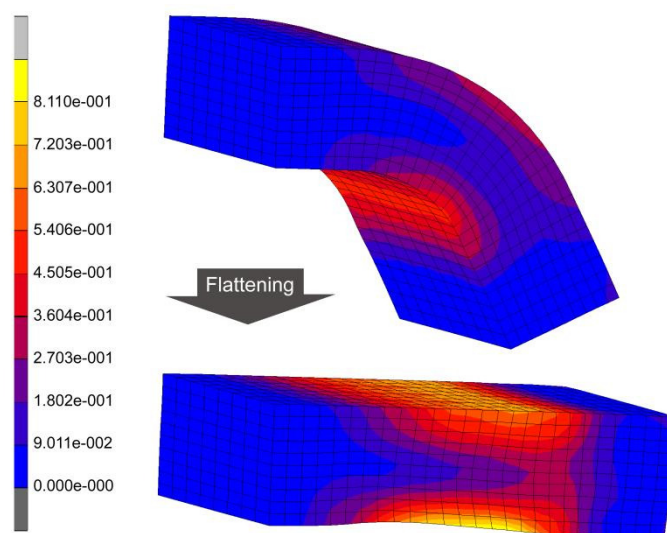

Fig. 5. Numerical prediction of total equivalent plastic strain from submodelling of Zone1, top: after CRF, bottom: after flattening.

3. Experimentation

3.1. Approach

In order to establish a basis for material study, Vickers Hardness test was implemented on the specimen. The focus in the measurements was the fold zones since they undergo large compressive and tensile plastic deformations. Depending on process parameters, a relatively severe gradient of plastic strain occurs in these regions that can lead to high level of hardening and damage due to micro defect nucleation and growth.

To study the effect of flattening, bents were unbent by compression between closing jaws of a bench vice and marked up for micro-indentation. The sample cross-sections were secured in the polymer mount and prepared using successive grinding and polishing. Fig. 6 shows the overview of the test specimens.
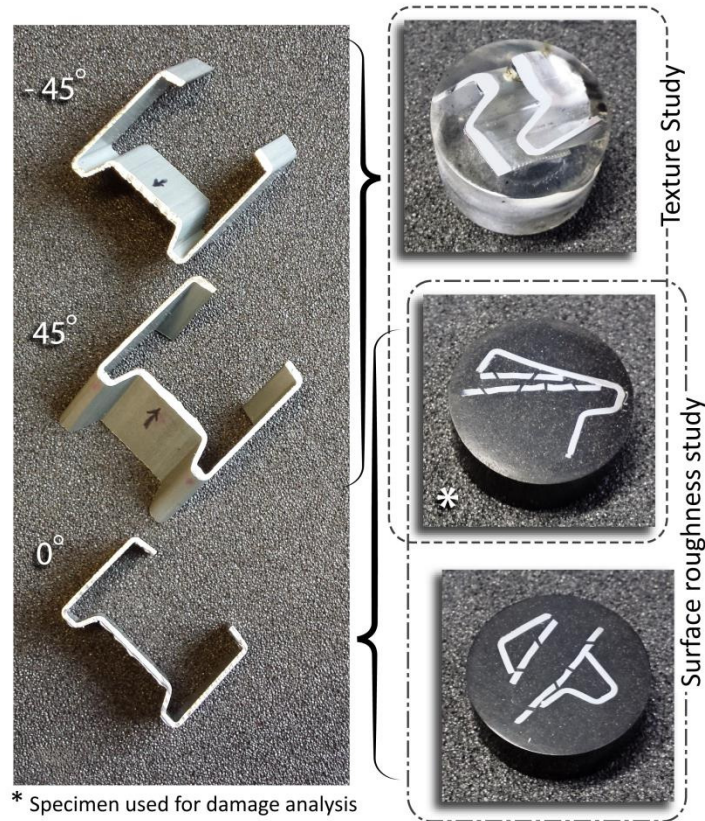

Fig. 6. Specimens used in the experiment for damage characterization and investigating the sensitivity of microhardness measurements to texture and surface roughness. Left: cut outs from roll formed profile. Right: samples mounted and polished for to test.

The multifunctional hardness tester of Micro Materials was adopted to test the hardness variation of the cross-section through a fine grid of micro-indentations on each region covering a reasonable area. In thickness direction, the grid consisted of 9 indents that covered as close as 50 µm to the edge of the sample. Vickers micro indenter was employed and the 500 mN load-controlled indentations were performed over 30 sec ramp.

To obtain a reference that serves to identify how the hardness evolves through manufacturing stages, a sample from the virgin sheet was used, mounted and polished. Microhardness test on the cross-section with several columns of indentation running from one side to the other. Fig. 7 shows the average of these results and depicts a non-uniformity of hardness in the thickness direction. In fact, material closer to the sheet

11

surface is harder. This could be due to the smaller grain size near the faces as the cooling rate is higher on the surface during the manufacturing process, consequently non-homogeneity in mechanical behaviour is induced. This observation is similar to through thickness hardness reported by Mkaddem et al. (2002). The subtle non-symmetry in the hardness graph seemed to be negligible.
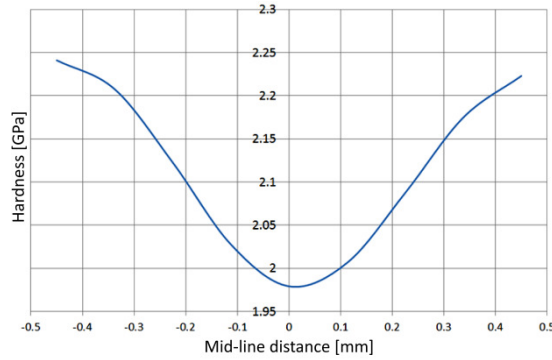

Fig. 7. Through thickness hardness measurement on virgin sheet.

In addition to virgin material, micro-indentation was carried out on fold zones to characterise the material's straining behaviour in plastic regime before and after flattening.

Fig. 8 shows the overlaid micro-hardness maps on investigated areas. Using the Gaussian filtering, the spikes were smoothed out.
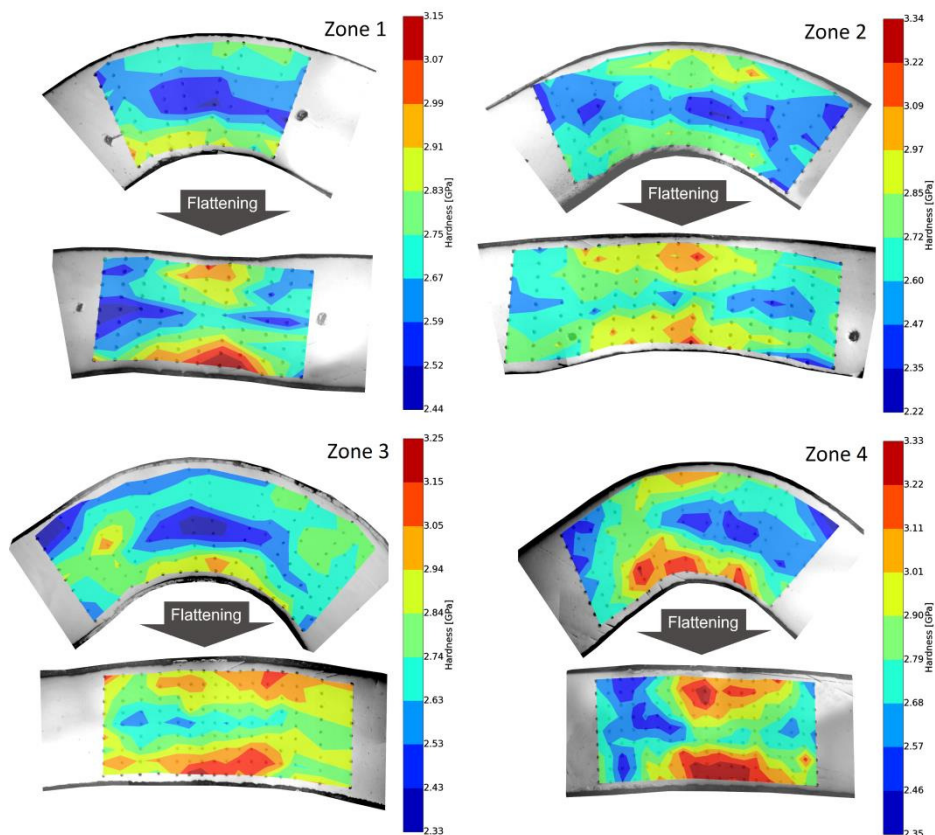
Fig. 8. Hardness field measured in four fold zones, after forming and after flattening.

Before damage analysis using the microhardness values, the influence of texture and surface roughness on the microhardness measurement was investigated. The significance of texture or crystallographic orientations to material lies in the fact that many material properties are texture-specific. Texture can influence the material properties 20-50% of the property value according to Engler and Randle (2009). This investigation was carried out by studying material behaviour on non-parallel planes. Therefore, cuts from the profile at -45° and 45° angles with reference to the normal cross-sectional plane were also tested (see Fig. 6).

Alongside sensitivity of microhardness to texture, two different surface finish of the normal cross section was also studied. Two set of tests were carried out; one with a poor surface finish (Ra=0.021µm) and the other with highly polished (Ra=0.006µm).

4.   Discussion and results

4.1.   Impact of texture and surface roughness on measurement

Fig. 9 depicts the hardness results obtained from all experiments in four zones for three planes at different angles as well as poor surface roughness. These graph shows the hardness picked up from a narrow band running through the thickness in the middle of bend corner. It can be seen that there is reasonably low variation between the hardness results obtained from different angles. This highlights the fact that the results are reliable and insensitive to texture. There is also a reasonably small uncertainty due to surface roughness as indicated in Fig. 9. It is seen that there is a marginal deviation caused by surface roughness which highlights the indentations are deep enough to get away with the adverse influences of poor surface finish discussed by Hu et al. (2013).
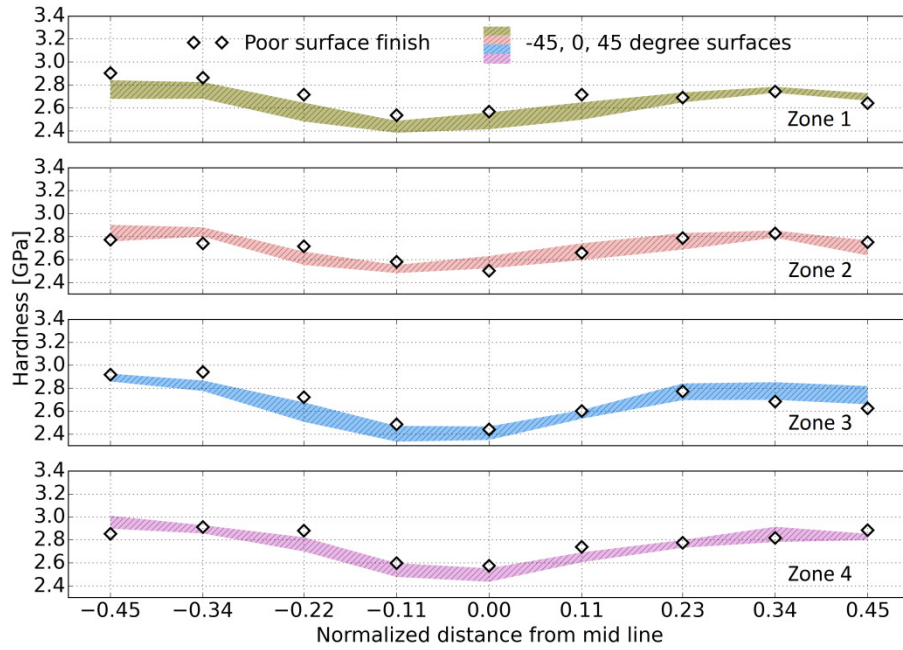
13

Fig. 9. Hardness results on bend zones. The shaded error bands shows the scatter in microhardness obtained from different cross-sectional cutting angle obtained from high quality surface finish (Ra=0.006µm). The diamond points are the results obtained from the specimen with poor surface finish (Ra=0.021µm).

4.2. Characterisation of damage

Micro hardness based ductile damage characterization is a non-direct method by which damage is measured through its effects on hardening properties. Amongst several methods such as, analysing variation of density, propagation of waves, electrical resistance change, acoustic emission, stiffness' and hardness, microhardness analysis appear to be the most promising Mkaddem et al. (2006).Lemaitre and Dufailly (1987) first introduced a correlation between the occurrence of damage and drop of the hardness in the material, using:

$$D = 1 - H_i/H_0 \tag{1}$$

Where D is damage parameter, H_i is the hardness of the damaged material which is actually measured and H_0 is the hardness of the same material in absence of damage, which is obviously a fictitious value. H_0 could be estimated using extrapolation. The technique employed in this study to calculate H_0 through the thickness of bend and unbent sheet material is the experimental hardness results in conjunction with FE simulation.

The correlation between micro-hardness, measured based on Vickers method and the yield stress σ_y has been studied by several researchers and reported to be proportional, i.e.:

14

$$HV = \alpha \, \sigma_y \tag{2}$$

The proportionality factor α has been outlined to be between 2.5 to 3.0. In order to take into account the strain hardening during the plastic deformation, σ_y is to be replaced by the current yield stress.

$$H = \alpha \, (\sigma_y{}^*) \tag{3}$$

$$\sigma_y{}^* = K \, \varepsilon_p^{*n} \tag{4}$$

$$\varepsilon_p^* = \varepsilon_p + \varepsilon_{offset} \tag{5}$$

Eventually hardness could be written as:

$$H = \alpha \, K (\varepsilon_p + \varepsilon_{offset})^{\,n} \tag{6}$$

In which ε_p is the plastic strain, H is the hardness (MPa), n and K are the hardening exponent and coefficient respectively. ε_{offset} is the offset to take into account the plastic strain induced due to indentation test as discussed by Tekkaya and Lange (2000). This offset was reported to be dependent on level of plastic strain in the material.

To do extrapolation the relationship presented in Eq. 6 is fitted to the experimental hardness and corresponding equivalent plastic strain through the thickness of the material. In this curve fitting however only the data points around the neutral axis are used where material is not highly deformed and still demonstrates a strain hardening trend. This relationship is then used to extrapolate the value of H_0 for regions where the material is highly deformed and probably damaged. Complete FE simulation of the actual forming process is deemed to have captured the intricate and complex deformation profile occurring through the actual process. The distribution of plastic deformation shows a trend similar to experimental microhardness map depicted in
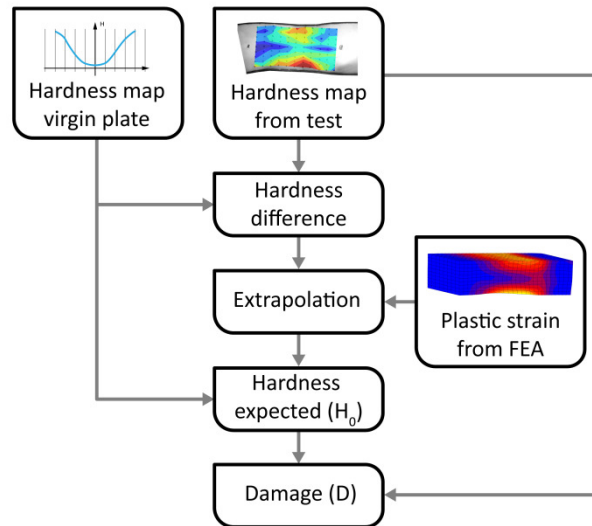
Fig. 8.

Fig. 10. Damage analysis flow diagram.

The process of calculating damage is shown as block diagram in Fig. 10. As mentioned earlier the hardness profile of the virgin material is an important part of the process. This data is used to work out hardness change in this technique due to plastic stain in the material. Extrapolation is then carried out and finally H_0 is calculated and used to determine damage. The result of damage quantification is shown in Fig. 11. In this figure the virtual hardness is shown as undamaged material, and then the difference between the two curves was regarded as a mean to analyse damage. Based on the measured microhardness and equivalent plastic strain, the proportionality value obtained through curve fitting was 2.9-3.1 which is inline the reported proportionality factors in the literature by Zhang et al. (2011) and Sonmez and Demir (2007).
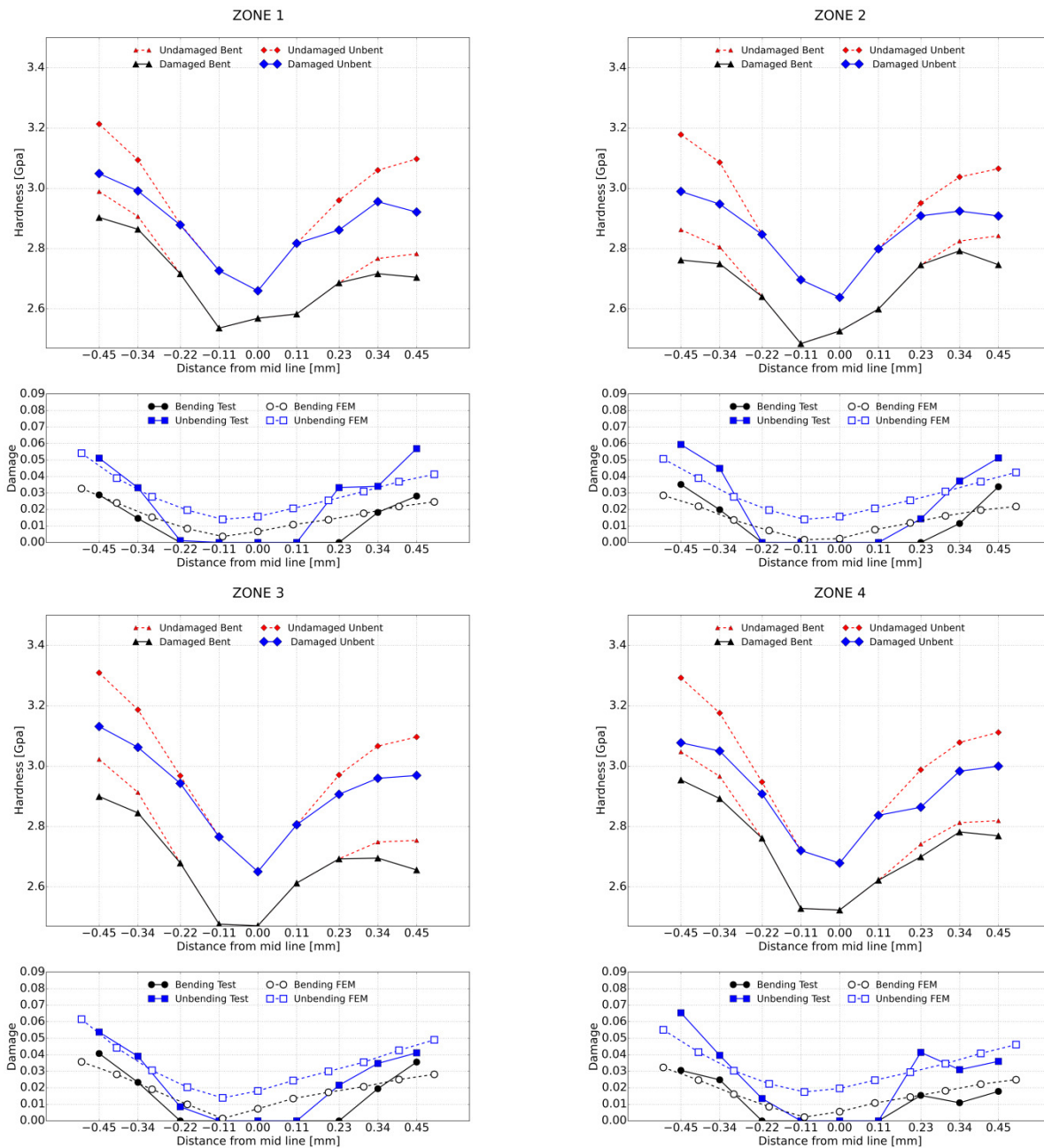
Fig. 11. Damage analysis of bending and flattening for zones 1-4. Innes side of the bend is demonstrated by negative values.

Fig. 11 shows several stages of forming hardened up the virgin material, however, there is a level of hardness beyond which the hardening process slows down and even material starts softening. The overall increase in the hardness after flattening, even around neutral axis, is due to compress flattening process in which unlike pure unbending the outer surface of the bend acts as hinge rather than the neutral axis.

Fig. 11 also shows the comparison of experimental result with the damage obtained from numerical simulation using Bonora model. Although both results are in the same domain, there are a few items to point out regarding their differences. The technique presented in this approach approximate the H_0 by curve fitting based on the strain and the hardness around the neutral axis. This of course masks the damage present in this region by assuming no gap between H_0 and H_i , especially in unbending experiment.

The results show damage in the inner side of the bend as well as outer side. This region is generally assumed to experience compression and hence not prone to damage evolution. The numerical simulation however demonstrate fluctuations of stress triaxiality between negative and positive values as the material sequentially undergoes forming stages and when come off them. This could partially explain why hardness drop is observed in inner side of the bend.

Assuming the $D_{cr} = 0.12$ according to Table 1, we can look at the material load bearing degradation as following equation:

$$Residual\ load\ bearing\ capacity = \frac{1}{n} \sum_{i=1}^{n} 1 - \left(\frac{D_i}{D_{cr}}\right) \tag{7}$$

In which i is the number of studied points through the thickness. Considering material failure at D_{cr} , the above equation speaks to the level of load bearing capacity given the strip with a flattened bend is weakest point. Table 2 shows the result obtained from experiment and FE simulation.

Table 2. Experimental and numerical residual load bearing capacity for all zones.

	Experiment		FEA	
	Bent	Flattened	Bent	Flattened
Zone 1	0.91	0.80	0.86	0.75
Zone 2	0.90	0.80	0.88	0.75
Zone 3	0.89	0.79	0.84	0.71
Zone 4	0.90	0.78	0.86	0.72

Given the fact that Takano et al. (2008) reported the important factor for restoration of material to original capacity is to restore the thickness, it could be implied that in absence of thickness recovery the presented values in Table 2 can address the residual load bearing capacity of a deformed material.

The flattening operation in this study imposed a localized deformation to the bend corners of CRF profile, and yet experimental and numerical assessments outlined around %70 residual load bearing capacity. These results suggest that even in presence of such inhomogeneity there is a significant potential for successful cold recycling.

5. Conclusions

The present study was an effort to promote sustainable manufacturing by presenting cold recycleability assessment for formed sheet metal. This numerical and experimental study was carried out by characterizing the material load carrying capacity after primary forming process. Assuming an intermediate flattening stage prior to the secondary forming process, additionally imposed degradation was also assessed after flattening.

Cold roll formed profile was picked up as case study and a new experimental method was demonstrated to characterize the damage of critical zones in thickness direction by using microhardness tests on the cross-section of the virgin and formed material, in conjunction with the FE simulation. Independent numerical damage identification delivered a well correlated assessment of the material degradation. The technique exhibited suitability for similar cases.

With emphasis on studying through thickness plastic deformation, a 3D simulation of cold roll forming process was required with multiple layers of solid elements. To address this challenge, submodelling technique was effectively employed to reduce computational cost in which the global/master was modelled using shell elements, followed by submodelling with layers of solid elements in fold zones.

In this study the sensitivity of experimental hardness to texture was also probed by performing measurement on cross-sections cut in three different angles. It was observed that the measured hardness was reasonably consistent and not sensitive to orientations. Further, effect of specimen surface finish quality was looked into. It was revealed that the microhardness measurements can be reliable in terms of sensitivity to surface finish.

The degradation observed due to forming highlighted the fact that given a suitable subsequent forming process after flattening, the material still could be used to an acceptable capacity.

19

References

Bidabadi, B.S., Naeini, H.M., Tehrani, M.S. and Barghikar, H., 2015. Experimental and numerical study of bowing defects in cold roll-formed, U-channel sections. Journal of Constructional Steel Research.

Bonora, N., 1997. A nonlinear CDM model for ductile failure. Engineering fracture mechanics 58, 11-28.

Bonora, N., Gentile, D., Pirondi, A., 2004. Identification of the parameters of a non-linear continuum damage mechanics model for ductile failure in metals. The Journal of Strain Analysis for Engineering Design 39, 639-651.

Bui, Q.V., Ponthot, J., 2008. Numerical simulation of cold roll-forming processes. Journal of Materials Processing Technology 202, 275-282.

Cooper, D.R., Gutowski, T.G., 2015. The Environmental Impacts of Reuse: A Review. Journal of Industrial Ecology.

Engler, O., Randle, V., 2009. Introduction to Texture Analysis: Macrotexture, Microtexture, and Orientation Mapping, Second Edition, Second ed. CRC Press.

Guo, Z.E.N.G., LAI, X.M., YU, Z.Q. and LIN, Z.Q., 2009. Numerical simulation and sensitivity analysis of parameters for multistand roll forming of channel section with outer edge. *Journal of Iron and Steel Research, International*, *16*(1), pp.32-37.

Heislitz, F., Livatyali, H., Ahmetoglu, M.A., Kinzel, G.L., Altan, T., 1996. Simulation of roll forming process with 3-D FEM Code PAM-STAMP. Journal of Materials Processing Technology 59, 59-67.

Hellborg, S., 2007. Finite element simulation of roll forming.

Hong, S., Lee, S. and Kim, N., 2001. A parametric study on forming length in roll forming. *Journal of Materials Processing Technology*, *113*(1), pp.774-778.

Hu, Z., Lynne, K.J., Markondapatnaikuni, S.P., Delfanian, F., 2013. Material elastic–plastic property characterization by nanoindentation testing coupled with computer modeling. Materials Science and Engineering: A 587, 268-282.

Joo, B., Lee, H., Kim, D. and Moon, Y., 2011, August. A study on forming characteristics of roll forming process with high strength steel. In The 8th International Conference and Workshop on numerical simulation of 3D seet metal forming processes (NUMISHEET 2011) (pp. 1034-1040).

Lemaitre, J., Dufailly, J., 1987. Damage Measurements. Engineering Fracturte Mechanics 28, 643-661.

Li, S.H., Zeng, G., Ma, Y.F., Guo, Y.J., Lai, X.M., 2009. Residual stresses in roll-formed square hollow sections. Thin-Walled Structures 47, 505-513.

Lindgren, M., 2007. Cold roll forming of a U-channel made of high strength steel. Journal of Materials Processing Technology 186, 77-81.

MARC, 2014. Volume B: Element Library. MSC Software Corporation, USA.

McClure, C.K., Li, H., 1995. Roll forming simulation using finite element analysis. Manufacturing Review 8, 114-122.

Mkaddem, A., Gassara, F., Hambli, R., 2006. A new procedure using the microhardness technique for sheet material damage characterisation. Journal of Materials Processing Technology 178, 111-118.

Mkaddem, A., Potiron, A., Lebrun, J.-L., 2002. Straightening and bending process characterization using Vickers micro hardness technique, International Conference of Advanced Technology of Plasticity, pp. 631-636.

Muller, M., Barrans, S.M., Blunt, L., 2011. Predicting plastic deformation and work hardening during V-band formation. Journal of Materials Processing Technology 211, 627-636.

Paralikas, J., Salonitis, K. and Chryssolouris, G., 2009. Investigation of the effects of main roll-forming process parameters on quality for a V-section profile from AHSS. The International Journal of Advanced Manufacturing Technology, 44(3-4), pp.223-237.

Paralikas, J., Salonitis, K. and Chryssolouris, G., 2010. Optimization of roll forming process parameters—a semi-empirical approach. The International Journal of Advanced Manufacturing Technology, 47(9-12), pp.1041-1052.

Park, J.C., Yang, D.Y., Cha, M., Kim, D. and Nam, J.B., 2014. Investigation of a new incremental counter forming in flexible roll forming to manufacture accurate profiles with variable cross-sections. *International Journal of Machine Tools and Manufacture*, *86*, pp.68-80.

Rossi, B., Degée, H. and Boman, R., 2013. Numerical simulation of the roll forming of thin-walled sections and evaluation of corner strength enhancement. *Finite Elements in Analysis and Design*, *72*, pp.13-20.

Safdarian, R. and Naeini, H.M., 2015. The effects of forming parameters on the cold roll forming of channel section. Thin-Walled Structures, 92, pp.130-136.

Sheu, J.-J., 2004. Simulation and optimization of the cold roll-forming process. AIP Conference Proceedings 712, 452-457.

Sonmez, F.O., Demir, A., 2007. Analytical relations between hardness and strain for cold formed parts. Journal of Materials Processing Technology 186, 163-173.

Takano, H., Kitazawa, K., Goto, T., 2008. Incremental forming of nonuniform sheet metal: Possibility of cold recycling process of sheet metal waste. International Journal of Machine Tools and Manufacture 48, 477-482.

Tasan, C.C., Hoefnagels, J.P.M., Geers, M.G.D., 2012. Identification of the continuum damage parameter: An experimental challenge in modeling damage evolution. Acta Materialia 60, 3581-3589.

Tehrani, M.S., Hartley, P., Naeini, H.M. and Khademizadeh, H., 2006. Localised edge buckling in cold roll-forming of symmetric channel section.Thin-walled structures, 44(2), pp.184-196.

Tekkaya, A., Lange, K., 2000. An improved relationship between Vickers hardness and yield stress for cold formed materials and its experimental verification. CIRP Annals-Manufacturing Technology 49, 205-208.

Tekkaya, A.E., Franzen, V., Trompeter, M., 2008. Wiederverwertungsstrategien für Blechbauteile, 15 SFU, Dresden, pp. 187-196.

Wiebenga, J.H., Weiss, M., Rolfe, B., van den Boogaard, A.H., 2013. Product defect compensation by robust optimization of a cold roll forming process. Journal of Materials Processing Technology 213, 978-986.

Zeng, G., Li, S., Yu, Z., Lai, X., 2009. Optimization design of roll profiles for cold roll forming based on response surface method. Materials & Design 30, 1930-1938.

Zhang, P., Li, S., Zhang, Z., 2011. General relationship between strength and hardness. Materials Science and Engineering: A 529, 62-73.